A secular variation candidate model for IGRF-14 combining observatory and satellite data with ensemble inverse geodynamo modelling

A. Fournier, J. Aubert, V. Lesur

Université Paris Cité, Institut de physique du globe de Paris, France

September 29, 2024

This document presents the methodology used by our group to design a secular variation candidate model for years 2025–2030. A geomagnetic field model centered around 2024.0 is first constructed, based on satellite and observatory data, for both the main field and its instantaneous secular variation (hereafter SV). This initial model and its uncertainties are next fed into an inverse geodynamo modelling framework in order to specify, for epoch 2024.0, an ensemble of 100 initial conditions for the integration of a three-dimensional numerical dynamo model. We use the ensemble of deterministic integrations between years 2025.0 and 2030.0 to propose a time-average secular variation model for that time frame (this SV model is thus centered on 2027.5), along with uncertainties deduced from the statistical properties of the ensemble.

Contents

Comp.	Type	ML	HL
X	Swarm A	9 nT^2	100 nT^2
Y	Swarm A	9 nT^2	81 nT^2
Z	Swarm A	16 nT^2	81 nT^2
X	Observ.	16 nT^2	36 nT^2
Y	Observ.	16 nT^2	25 nT^2
Z	Observ.	25 nT^2	36 nT^2

Table 1: Variances prescribed to the three components of mid-latitude (ML) and high-latitude (HL) vector data.

1 Construction of the initial model

The initial model is constructed according to the method detailed by Ropp and Lesur (2023).

1.1 Data selection

We consider vector data from Oersted, CHAMP, CryoSat-2 and Swarm satellite A to cover epochs from 1999.0 to 2024.5. Over the same period, we also used hourly mean vector observatory data. (We dot not utilize magnetic intensity data.) For the Swarm data we use systematically the latest versions available of the SW_OPER_MAGA_LR data, namely version 0605 or version 0606.

Data selection differs depending on the geomagnetic latitude. We distinguish high-latitude (HL henceforth) data from mid-latitude (ML henceforth) data. HL (resp. ML) data correspond to a geomagnetic latitude of absolute value larger (resp. smaller) than 55°.

The following selection criteria apply:

- ML data are selected for local times between 11:00 pm and 5:00 am, and rejected for sunlit ionosphere.
- Data are selected for positive values of the vertical component of the interplanetary magnetic field (IMF): $B^Z_{IMF} > 0$.
- Data are selected for D_{st} values inside $[-30 : 30]$ nT and its time variation $\dot{D}_{st}$ between $[-100 : 100]$ nT/day: we are interested in the low-frequency component of the signal measured during quiet times.
- ML satellite data are sampled every 30 seconds, while HL satellite data are sampled every 60 seconds. This corresponds to collecting one point approximately every degree along the satellite track.

The size of the corresponding data vector is very large and for year 2024 only reaches 48453 (=3×16151) ML satellite data, 53343 HL satellite data and 33390 observatory data. Note that HL data are handled in the usual North, East, Center (NEC) reference frame, whereas ML data are used in a Solar Magnetic (SM) reference frame, reducing this way the correlations between vector data component errors.

1.2 Data weights

The variances attributed to each type of data are given in Table 1. The inverse of the variance is used to weigh the data when constructing the initial model.

1.3 Modelling method and initial model parameterization

The derived model consists of a series of snap-shot models, 365.25/4 days apart, estimated from 1999 to 2025 using a Kalman filter, with smoothing, in a similar way as the process used in Ropp and Lesur (2023). The data for each snap-shot are fitted through a robust re-weighted iterative least-squares process, using Huber weights. The first iteration is a standard L_2-norm least-squares inversion.

The magnetic field potential V is represented using a spherical harmonic expansion of the form

$$\begin{aligned} V(r,\theta,\varphi,t) &= V_i(r,\theta,\varphi,t) + V_e(r,\theta,\varphi,t) \\ &= a\sum_{\ell=1}^{L_i}\left(\frac{a}{r}\right)^{\ell+1}\sum_{m=0}^{\ell}\left[g_\ell^m(t)\cos(m\varphi) + h_\ell^m(t)\sin(m\varphi)\right]\mathcal{P}_\ell^m(\cos\theta) \\ &+ a\sum_{\ell=1}^{L_e}\left(\frac{r}{a}\right)^{\ell}\sum_{m=0}^{\ell}\left[q_\ell^m(t)\cos(m\varphi) + s_\ell^m(t)\sin(m\varphi)\right]\mathcal{P}_\ell^m(\cos\theta)\,, \end{aligned}$$

in which (r,θ,φ) denote the standard spherical coordinates, t is time, a is the mean radius of the Earth (a = 6371.2 km), L_i is the truncation of the spherical harmonic expansion of the internal sources, and L_e the truncation of the expansion of the external sources. The $\mathcal{P}_\ell^m$ are the associated Legendre functions of degree ℓ and order m, whose normalization is subject to the Schmidt convention.

The description of internal and external sources is done in the same way as in Ropp and Lesur (2023). The idea is essentially to over-parameterize the contribution of each source and to constrain the resulting parameters using physical prior information as described in Holschneider et al. (2016). Although it influences little the derived core field model, we point that the core surface flow is co-estimated together with the magnetic field model.

Prior information on the model components is provided through the description of a Gaussian model distribution characterized by a mean and a covariance matrix. For all model sources the mean is zero. The prior information used to constrain the core field and SV Gauss coefficients is based on the multivariate statistics of a 70,000 year long free run integration of the coupled Earth dynamo model by Aubert et al. (2013). This choice is motivated by the will to ensure consistency between the initial model and the forecast that is produced using the same numerical model (more on the forecast below).

1.3.1 Internal sources

The truncation applied for internal sources is $L_i = 30$. The main (dynamo) field is described up to spherical harmonic degree 18, and so is its secular variation. The crustal field is expanded in spherical harmonic degree from degree 15 to degree $L_i = 30$ (prior covariance properties: radius 6280.0 km, scaling factor= 2.7 10^{-2}). A known crustal field (Lesur et al., 2013) is subtracted from the data for degrees 30 to 110.

The induced mantle field is described by two parts:

- for each snap-shot up to spherical harmonic degree 6 a static and a linearly varying components. (prior covariance properties: radius=3485 km, scaling factors= 5 and 160 respectively)
- for each snap-shot up to spherical harmonic degree 3 a component proportional to the D_{st} index. (prior covariance properties: radius=2537 km, scaling factor= 1)

Crustal offsets are co-estimated for observatory data as 3 constants per observatory (prior covariance properties with a radius given y the observatory altitude and a scaling factor equal to 10000).

1.3.2 External sources

The external sources considered are the following:

- A static external field in the Geocentric Solar Magnetopsheric (GSM) coordinate system for the remote magnetosphere (prior covariance properties: radius= 16000 km, scaling factor= 5400)
- A static external field in the Solar magnetic (SM) coordinate system for the near magnetosphere (prior covariance properties: radius=6900 km, scaling factor=3.56)
- A time-varying external field dependent upon the external D_{st} index (prior covariance properties: radius=16 000 km, scaling factor= 5.4)
- A time-varying external field dependent on the Y component of the IMF in the SM coordinate system (prior covariance properties: radius=6 900 km, scaling factor= 0.1)

Each of these external sources is described up to spherical harmonic degree $L_e = 3$.

1.3.3 The initial model

The initial model, centered on 2024.0, is obtained after 105 iterations of the Kalman filter, followed by a smoothing process. Of particular interest for the prediction of the SV to be described below are the sets of Gauss coefficients of the main field and its SV at epoch 2024.0, along with their associated posterior covariance matrices $\mathbf{C}_{\mathrm{MF}}$ and $\mathbf{C}_{\mathrm{SV}}$, respectively.

2 Ensemble-based inverse geodynamo modelling

Our approach is identical to the one followed for our contribution to IGRF-13 (Fournier et al., 2021). With the initial model (and its error covariance matrices $\mathbf{C}_{\mathrm{MF}}$ and $\mathbf{C}_{\mathrm{SV}}$) at hand, we next apply the inverse geodynamo modelling framework of Aubert (2014) with a few novel features, namely an ensemble approach to deal with uncertainties and the possibility to enforce a QG-MAC force balance for the initial condition to be prescribed (Aubert, 2020). The numerical dynamo model we resort to is the coupled Earth dynamo (Aubert et al., 2013).

The multistep approach can be summarized as follows:

1. 100 decorrelated independent dynamo states are extracted from a 70,000 year long free run integration of the coupled Earth Dynamo.
2. For each ensemble member e, a Kalman filter estimates the three-dimensional structure of the magnetic field $\mathbf{B}_e$(dyn,3D) in the core interior from the field provided by the initial model $\mathbf{B}$(obs) and the prior information based on the statistics (mean and covariance) of the 70,000 year long free run integration.
3. For each ensemble member e, the knowledge of the three-dimensional magnetic structure inside the core makes it possible to compute the three-dimensional magnetic diffusion inside the core, $\mathbf{D}_{\mathrm{mag},e}$.
4. We next solve a diffusion-free core-flow problem at the core surface, seeking the core surface field $\mathbf{u}_{s,e}$ which satisfies

$$\hat{\boldsymbol{r}} \cdot \left[\dot{\mathbf{B}}(\mathrm{obs}) - \mathbf{D}_{\mathrm{mag},e} \right] = -\boldsymbol{\nabla}_h \cdot \left(\mathbf{u}_{s,e}\, \hat{\boldsymbol{r}} \cdot \mathbf{B}_e(\mathrm{dyn,3D}) \right),$$

   where $\hat{\boldsymbol{r}}$ is the unit vector in the spherical radial direction. This problem is solved under the weak constraint that the QG-MAC balance is satisfied at the core surface (Aubert, 2020).

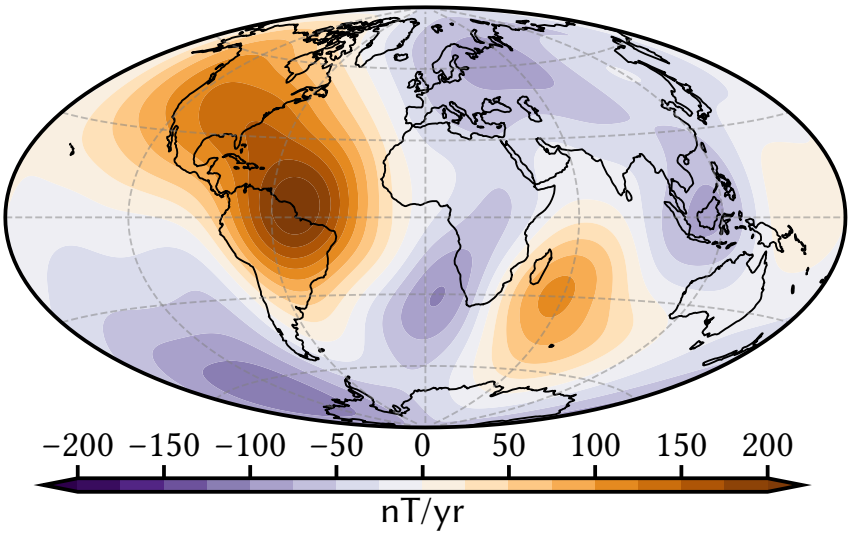

Figure 1: Radial component of the average secular variation (truncated at spherical harmonic degree 8) at Earth's surface for the 2025 – 2030 period. Hammer projection.

5. Finally, another Kalman filter converts this estimate of $\mathbf{u}_{s,e}$ into a three-dimensional estimate of the flow and buoyancy fields, for this member of the ensemble.

The three-dimensional estimates of the buoyancy, magnetic field and flow define a unique initial condition for the integration of the numerical dynamo model, details of which can be found in the study of (Aubert et al., 2013, and references therein). This integration is performed for each ensemble member e. Note that we assumed that the flow was steady over the 2024 – 2030 period, in line with the strategy we followed for IGRF-13 (consult Fournier et al., 2021, for details).

3 Secular variation candidate

3.1 Definition

For each ensemble member e, we compute

$$\frac{\mathbf{B}_e(t = 2030.0) - \mathbf{B}_e(t = 2025.0)}{5 \text{ years}}$$

at the surface of the Earth (mean spherical radius 6371.2 km). Our candidate model is the median of this ensemble of average SV predictions. This candidate is shown in Figure 1.

3.2 Uncertainties

The uncertainties are given by the 90% credible interval for each Gauss coefficient of the ensemble of 100 predicted SV.

References

Aubert, J. (2014). "Earth's core internal dynamics 1840–2010 imaged by inverse geodynamo modelling". In: *Geophysical Journal International* 197.3, pp. 1321–1334.

— (2020). "Recent geomagnetic variations and the force balance in Earth's core". In: *Geophysical Journal International* 221, pp. 378–393. DOI: 10.1093/gji/ggaa007.

Aubert, J., C. C. Finlay, and A. Fournier (2013). "Bottom-up control of geomagnetic secular variation by the Earth's inner core". In: *Nature* 502, pp. 219–223. DOI: 10.1038/nature12574.

Fournier, A., J. Aubert, V. Lesur, and G. Ropp (2021). "A secular variation candidate model for IGRF-13 based on Swarm data and ensemble inverse geodynamo modelling". In: *Earth, Planets and Space* 73, p. 43. DOI: 10.1186/s40623-020-01309-9.

Holschneider, M., V. Lesur, S. Mauerberger, and J. Baerenzung (2016). "Correlation-based modeling and separation of geomagnetic field components". In: *Journal of Geophysical Research: Solid Earth* 121.5, pp. 3142–3160. DOI: 10.1002/2015JB012629.

Lesur, V., M. Rother, F. Vervelidou, M. Hamoudi, and E. Thébault (2013). "Post-processing scheme for modeling the lithospheric magnetic field". In: *Solid Earth* 4, pp. 105–118. DOI: 10.5194/sed-4-105-2013.

Ropp, G. and V. Lesur (2023). "Mid-latitude and equatorial core surface flow variations derived from observatory and satellite magnetic data". In: *Geophysical Journal International* 234.2, pp. 1191–1204. DOI: 10.1093/gji/ggad113.

Acknowledgements This work was partly supported by the CNES grants 'Suivi et exploitation de la mission Swarm' and 'Kourou observatory' projects and by ESA (contract 4000109587/13/I-NB Swarm ESL/SW-CO-DTU-GS-010). This modelling work would not be possible without the contributions from observers in ground magnetic observatories and the work of the INTERMAGNET organization. Numerical computations were performed on the S-CAPAD/DANTE platform, IPGP, France.